Document downloaded from:

http://hdl.handle.net/10251/117019

This paper must be cited as:

Santiago-Portillo, A.; Garcia-Baldovi, H.; Carbonell Llopis, EJ.; Navalón Oltra, S.; Alvaro Rodríguez, MM.; García Gómez, H.; Ferrer Ribera, RB. (2018). Ruthenium(II) Tris(2,2'-bipyridyl) Complex Incorporated in UiO-67 as Photoredox Catalyst. The Journal of Physical Chemistry C. 122(51):29190-29199. https://doi.org/10.1021/acs.jpcc.8b07204

The final publication is available at

http://doi.org/10.1021/acs.jpcc.8b07204

Copyright American Chemical Society

Additional Information

Ruthenium(II) Tris (2,2'-bipyridyl) Complex Incorporated in UiO-67 as Photoredox Catalyst

Andrea Santiago-Portillo[a], *Herme G. Baldoví*[b], *Esther Carbonell*[c], *Sergio Navalón*[a], *Mercedes Álvaro*[a], *Hermenegildo García,*[*b] *Belén Ferrer*[* a]

[a] Departamento de Química, Universitat Politécnica de Valencia, Camino de Vera s/n, Valencia 46022, Spain.

[b] Instituto Universitario de Tecnología Química, CSIC-UPV, Universitat Politécnica de Valencia, Av. de los Naranjos, Valencia 46022, Spain.

[c] CMA Laboratory, Université de Namur, Rue de Bruxelles 61, 5000 Namur, Belgique

ABSTRACT. Ruthenium(II) bis(2,2'-bipyridine) (2,2'-bipyridyl-5,5'-dicarboxylic acid), Rudcbpy, attached to UiO-67(Zr) MOF, generates upon visible light excitation the localized triplet excited state of the ruthenium(II) bipyridyl complex that decays partly to very long-lived (millisecond time scale) photoinduced charge separated state following a similar behavior as that of analogous ruthenium(II) tris(bipyridyl) complex dissolved in water, except that the lifetime of soluble complex excited state is orders of magnitude shorter. The occurrence of photoinduced

charged separation on Rudcbpy-UiO-67(Zr) MOF has been proven visually by using methyl viologen as electron acceptor. Rudcbpy-UiO-67(Zr) behaves as a heterogeneous, reusable, photoredox catalyst promoting debromination of α-bromoketones with excellent selectivity at high conversions. Characterization data shows that Rudcbpy-UiO-67(Zr) is stable under the photocatalytic reaction conditions.

1. INTRODUCTION

Metal organic frameworks (MOFs) are crystalline porous materials where nodes constituted by metal ions or clusters of a few metal atoms are held in place by coordination with rigid bi- or multipodal organic linkers.[1-5] The strict ordering of the crystal lattice and the confined space provided by the internal pore volume of MOFs offer unique opportunities to perform photochemical processes in confined spaces that could exhibit features distinctive from the same process in homogeneous phase.[6-8] In addition, the versatility of MOF synthesis and design allows post-synthetic modification to build the target chromophores inside the solid pores, thus, making MOFs appealing materials for photochemical and optoelectronic applications.[9-17] For instance, photoexcitation of organic linkers in MOFs can lead to the generation of delocalized excitons with character of charge separate state by electron transfer from the linker to the metal node. These charge separated states can be characterized by their corresponding transient absorption spectra.[6,10,18]

The development of photoresponsive MOFs is a topic of large interest that can serve to obtain highly active photocatalyst for pollutant degradation [19-20] and solar fuel productions among other applications.[21-24] It would be important to go beyond these two areas to develop also photocatalysts for general organic transformation.[25-27]

Ruthenium(II) polypyridyl complexes are among the best studied molecules to promote photoinduced electron transfer (PET) reactions upon visible light irradiation.[27-31] The photophysics of ruthenium(II) polypyridyl complexes has been studied in virtually all conditions and also encapsulated inside different porous materials, including zeolites and mesoporous aluminosilicates.[32-34] These complexes typically present a metal-to-ligand charge transfer (MLCT) absorption band in the visible region that upon excitation leads to the generation of a triplet excited state in which an electron from Ru(II) migrates to the LUMO orbitals of the pyridyl ligands. This triplet excited state decays generally in the microsecond time scale and can be easily detectable by its characteristic phosphorescence. In the case of the most studied ruthenium(II) tris-2,2'-bipiridyl the absorption maximum of the MLCT band appears at 420 nm and the phosphorescence emission maximum at 620 nm. In the presence of electron acceptor or donor molecules, the triplet excited state of ruthenium(II) polypyridyl can donate or accept with high efficiency one electron forming the corresponding ruthenium(III) or ruthenium(I) polypyridyl complexes, respectively, that can be characterized by their corresponding absorption spectrum.[35]

In recent precedents to the present study, Lin and coworkers have prepared and characterized a ruthenium(II) trisbipyridyl complex grafted to the lattice of UiO-67(Zr).[36] Since the biphenyl-4,4'-dicarboxylate linker has the same size and directionality as 2,2'-bipyridyl-5-5'-dicarboxylate (dcbpy), there was a possibility to prepare a mixed ligand

biphenyl/Ru(II)(bpy)$_2$(dcbpy) UiO-67(Zr) MOF. Later, Morris and coworkers have studied the photophysics of a Ru(II)(bpy)$_2$(dcbpy)-doped UiO-67(Zr) MOF by emission spectroscopy and found that the steady-state emission and the emission lifetime of the MOF depend on the proportion of the ruthenium complex doping.[37-40] Chen and co-workers went a step further and took advantage of the photophysics of attached Ru polypyridyl complex to prepare a Ru-Pt@UiO-67 MOF containing Pt nanoparticles inside the pores of Ru(II)(bpy)$_2$(dcbpy)-doped UiO-67(Zr) that was employed as photocatalyst for hydrogen evolution from aqueous solution.[41]

Further information on the fate and behavior of the triplet excited state of the ruthenium polypyridyl complex can be obtained by following the evolution of this complex excited state by transient absorption spectroscopy (TAS) that can detect not only the triplet excited state of the Ru(II) complex, but also can determine the generation and evolution of non-emissive species and, particularly, the occurrence of PET. However, up to now, no TAS studies on Ru(II)(bpy)$_2$(dcbpy)-doped UiO-67(Zr) have been reported, even though TAS studies could detect spectroscopically species resulting from the PET that have so far not been characterized in MOFs.

The present work complements the existing reported photophysical data using TAS and provides some practical application by developing an efficient photocatalyst for photoredox organic transformation. Mechanistic insights based on TAS measurements support the occurrence of PET which is in agreement with the known behavior of Ru(II) polypyridyl complexes. The extremely long-lived charge separated state photogenerated on the Rudcbpy-UiO-67(Zr) MOF upon selective excitation of the Rudcbpy complex, detected and characterized here, provides a convincing evidence on the mechanism of the Rudcbpy-UiO-67 MOF as photocatalyst to carry out organic transformations,[36,42] and as semiconductor in general.[39]

2. EXPERIMENTAL SECTION

All chemicals and solvents including $RuCl_3 \cdot xH_2O$ (38−42% Ru), 2,2′-bipyridine (bpy, 99%), 2,2′-bipyridyl-5,5′-dicarboxylic acid (dcbpy, 95%), 4,4′-biphenyldicarboxylic acid (bpdc, 98%), $ZrCl_4$ (98%), $ZrOCl_2$ (99,99%), CH_3COOH (100 %), DMF (>99%), methanol (MeOH, >99%), ethanol (EtOH) and benzoic acid (BZA, 99%) were used as obtained without further purification from either Fisher Scientific or Sigma-Aldrich.

Preparation of Ru(II) Bis(2,2′-bipyridine)(2,2′-Bipyridyl-5,5′-dicarboxylic acid) dichloride, Rudcbpy. Ru(II) bis(2,2′-bipyridine) dichloride, $Ru(bpy)_2Cl_2$, was synthesized following the procedure described by Sullivan et al.[43] $Ru(bpy)_2Cl_2$ (0.160 g, 0.33 mmol) and dcbpy (0.101 g, 0.42 mmol) were suspended in 20 mL of EtOH-water and heated at reflux under N_2 all night. The solvent was then removed and the product was crystallized from MeOH/diethyl ether.[44]

Preparation of UiO-67(Zr). UiO-67(Zr) was synthesized following the procedure described by Morris et al.[37] 0.13 g of $ZrCl_4$ (0.56 mmol) and 3.4 g of BZA (28 mmol, 50 mol equiv) were dissolved in 20 mL of DMF by sonication for 10 min. This solution was added to a scintillation vial (20 mL) containing 0.14 g of bpdc (0.58 mmol). The mixture was sonicated for 10 min and then heated at 120 °C for 2 days. The mixture was cooled at room temperature and the crystalline white powder was filtered and washed three times with DMF (20 mL) and acetone (20 mL). Finally, the white powder was dried at air.

Preparation of Rudcbpy-UiO-67(Zr). Rudcbpy-UiO-67(Zr) was prepared following the procedure described above for the preparation of UiO-67(Zr) but with the addition of 50 mg of Rudcbpy together with the bpdc.

Synthesis of $Zr_6O_4(OH)_4$ cluster: 5 mL of 1.0 M $ZrOCl_2$ were mixed with 5 mL of 1 M CH_3COOH. The initial pH of 0.30 was increased to 1.77 by adding 2 M ammonium acetate solution.

Experimental conditions for the photo-generation of $MV^{\cdot+}$: 200 µl of an acetonitrile suspension of Rudcbpy-UiO-67 MOF (0.2 mg/ml), 1 ml of an acetonitrile solution of $MV(PF_6)_2$ 0.17 M and 50 µl of triethanolamine (TEOA) were introduced in a 10 mm × 10 mm quartz cell. 1.75 ml of acetonitrile was added in order to get a total volume of 3 ml. A standard acetonitrile solution of the Rudcbpy complex was prepared adding the same amounts of $MV(PF_6)_2$ and TEOA. The absorbance of the two solutions was adjusted to 0.3 at 532 nm. The solutions were bubbled for 15 min with argon and then irradiated for 10 min with a 532 nm laser beam through quartz.

Experimental conditions for the photoredox catalysis: The required amount of Ru complex (0.01 mmol of Ru) was introduced in a Pyrex tube with 2-bromoacetophenone (1 mmol) dissolved in acetonitrile (3 mL) and with TEOA (0.1 mL). The reaction was stirred magnetically at room temperature and irradiated with a medium pressure Hg lamp 125 W cooled through a quartz housing. The course of the reaction was periodically followed by extracting aliquots of the reaction mixture with a syringe, diluting in acetonitrile and injecting the mixture immediately in GC (6890 Network GC system Agilent technologies) and using a calibration plot to determine the product concentration. In the case of heterogeneity study, a filtration test was carried out. In this case, 1.5 mL of the reaction phase was filtered with a Nylon filter and the reaction of the liquid phase was followed by GC. Catalyst reusability was studied for Rubcdpy-UiO-67(Zr). In this experiment, the solid catalyst was recovered at the end of the reaction, at 2 h, by filtration in a Nylon filter (0.2 µm) and washed with more acetonitrile, water and ethanol and dried in an oven at 100 ºC. Then, the solid was used in a new catalytic cycle.

Characterization techniques: UV-visible spectra have been recorded in a Jasco-650 spectrophotometer. Diffuse reflectance UV-visible spectra were recorded on a Cary 5000 Varian spectrophotometer having an integrating sphere. Emission spectra were recorded in a Jasco 8500 spectrofluorimeter. X-ray powder diffraction (XRPD) data was measured on a Bruker PANanalytical Empyrean diffractometer (CuKα radiation) in transmission geometry. N_2 adsorption isotherms at 77 K were recorded by using a Micromeritics ASAP 2010 instrument. Thermogravimetric analyses were performed by using a TGA/SDTA851e METTLER TOLEDO station. H^1-NMR spectra were recorded in a Bruker Avance III 400 equipment (400 MHz).

Photophysical measurements: Laser flash photolysis measurements were carried out using the second harmonic of a Q switched Nd:YAG laser (Quantel Brilliant, 532 nm, 40 or 20 mJ/pulse, 5 ns fwhm) coupled to a mLFP-122 Luzchem miniaturized detection equipment. This transient absorption spectrophotometer consists of a 300 W ceramic xenon lamp, 125 mm monochromator, Tektronix TDS-2001C digitizer, compact photomultiplier and power supply, solid cell holder, fiber-optics connectors and computer interfaces. The software package was developed in the LabVIEW environment from National Instruments. The laser flash photolysis equipment supplies 5 V trigger pulses with programmable frequency and delay. The rise time of the detector/digitizer is ~3 ns up to 300 MHz (2.5 GHz sampling). The monitoring beam is provided by a ceramic xenon lamp and delivered through fiber-optic cables. The laser pulse is probed by a fiber that synchronizes the LFP system with the digitizer operating in the pretrigger mode. Transient spectra of the powders were recorded using 2×10 mm quartz cells and were bubbled for 15 min with argon or the corresponding quenching gas before data acquisition. Each decay or data point corresponds to the average of 10 signals to increase the signal to noise ratio.

For analysis of the experimental transient spectra of Rubcdpy-UiO-67(Zr) at long delay times, two different set of spectra have been employed. In one of them, the difference absorption spectra of UiO-67(Zr) after and before addition of Mg as strong reducing agent was taken as that of the spectrum of electrons at the nodes of UiO-67(Zr), assuming to be the same as those of Rubcdpy-UiO-67(Zr). In the other one, the spectrum of holes located at the bpdc ligands of Rubcdpy-UiO-67(Zr) was considered to be the transient absorption spectrum of UiO-67(Zr) after 266 nm excitation. It has been determined that the electrons in this UiO-67(Zr) are readily quenched by coadsorbed water present in the material. These spectra as well as the sum of the two are presented in Figure S16 and compared with the transient spectrum at long delay times recorded for Rubcdpy-UiO-67(Zr).

3. RESULTS AND DISCUSSION

3.1. Material preparation

The Rudcbpy-UiO-67(Zr) MOF has been synthesized as previously reported by Morris et al.[37] following a procedure similar to that described for the synthesis of parent UiO-67(Zr), but with the addition of 50 mg of Rudcbpy, together with the corresponding amount of bpdc, that should become incorporated in the framework during the formation of the crystal. XRD patterns, BET surface area, thermogravimetric analysis, diffuse reflectance absorption and emission spectra (see Supporting Information) are in excellent agreement with those results reported by Morris and Wang.[36-37] As an example to illustrate some of the characterization data of Rudcbpy-UiO-67(Zr) MOF, Figure 1 shows a comparison of the XRD pattern of this material with that of parent UiO-67(Zr). Further characterization data are provided on the supporting information. The Ru loading determined by ICP-OES analysis of the Rudcbpy-UiO-67(Zr) MOF after dissolution

in HNO_3 was 2 % which indicates that most of the Rudcbpy added in the initial solution has been incorporated into the MOF structure.

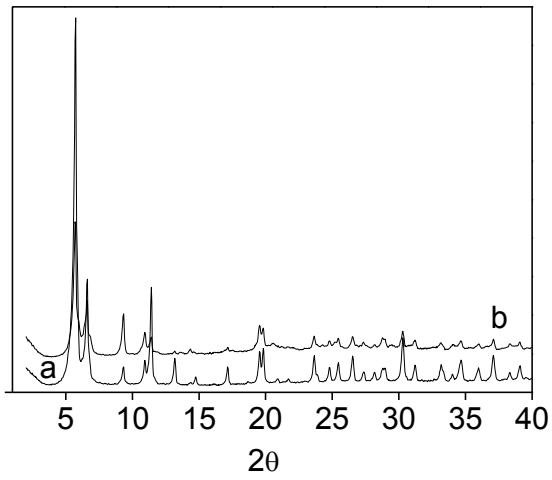

Figure 1. XRD patterns of UiO-67(Zr) (a) and Rudcbpy-UiO-67(Zr) (b).

3.2 TAS measurements

To characterize the photogenerated species upon selective Ru(II) polypyridyl excitation, TAS measurements of the powdered sample were performed and the signal monitored by the diffuse reflectance mode. Upon excitation at 532 nm, which ensures the selective excitation of the Ru polypyridyl complex, a transient absorption spectrum could be recorded. Its features depend on the monitoring time scale. At short time after the laser pulse (< 2.5 μs), the spectrum shows an absorption band centered at 350 nm and two negative signals centered at 460 and 680 nm, the latter being very strong (Figure 2). These signatures are those corresponding to the triplet excited state absorption of the Ru^{2+} polypyridyl (absorption band at 350 nm), the bleaching of the ground

state (negative signal at 460 nm) and the emission (negative signal at 640 nm), respectively. The temporal profiles of the transient signals monitored at 460 and 600 nm at short time scale are shown in Figure S7. From 2.5 to 20 μs after the laser pulse, there is still bleaching of the ground state, but a positive absorption band from 500 to 800 nm, centered at 680 nm, develops (Figure 2 and S7-S8). This means that the triplet excited state of $Ru^{2+|3}$ has decayed, as indicated by the lack of emission, but the ground state has not been fully recovered (negative signal corresponding to the ground state absorption) and there is still some intermediate Ru species involved in the transient signals. At longer time scales after the laser pulse, 500 μs, the bleaching of the ground state cannot be longer observed, but there is a shift towards shortest wavelengths in the maximum of the absorption band around 350 nm and there is still a positive absorption band centered 680 nm present in TAS (Figure 3). In a typical Ru polypyridyl complex transient spectrum in homogeneous phase, the positive transient signal decay monitored at 340 nm, attributable to the absorption of the triplet excited state $Ru^{2+|3}$, coincides with the growth of negative transient signal monitored at 450 nm, attributed to the bleaching of the ground state, indicating that the triplet excited state returns to the ground state by emissive and non-emissive interconversion system deactivation.[28-30]

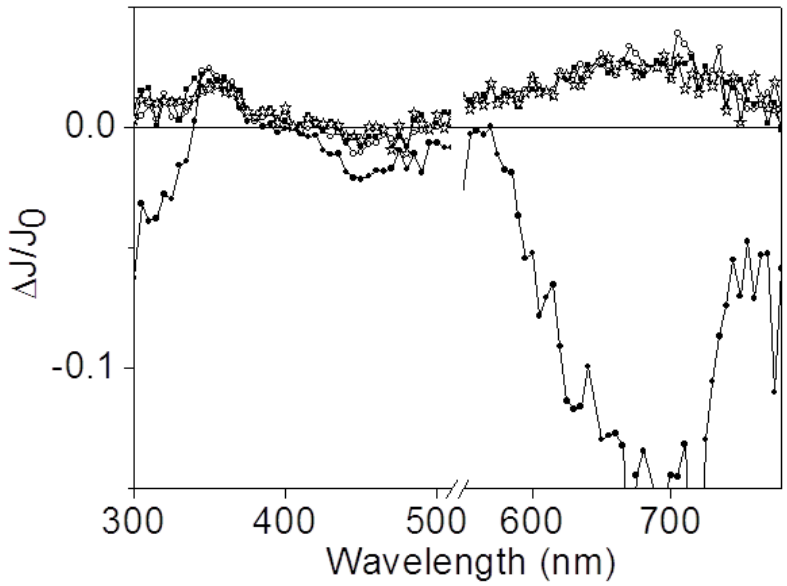

Figure 2. Diffuse reflectance transient absorption spectra of Rudcbpy-UiO-67(Zr) MOF recorded 1 (●), 6 (❍), 20(■) and 40 (✧) μs upon 532 nm laser excitation under argon atmosphere.

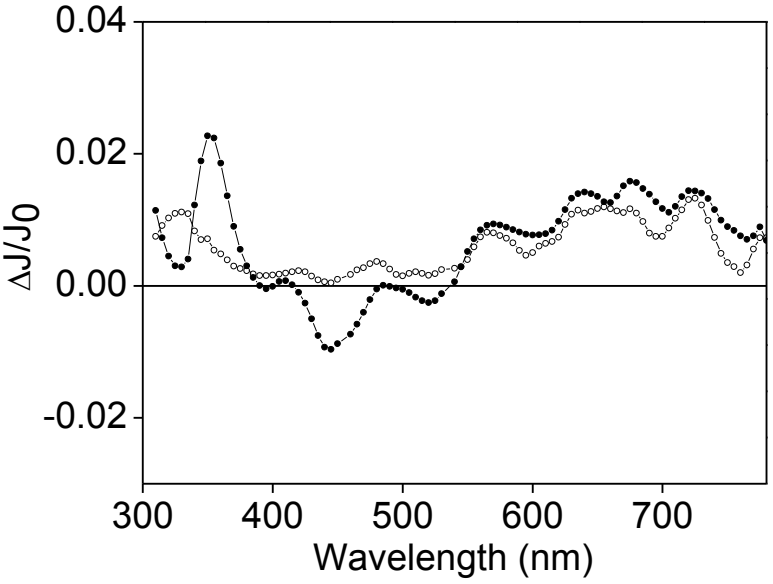

Figure 3. Diffuse reflectance transient absorption spectra of Rudcbpy-UiO-67(Zr) MOF recorded 20 (●) and 500 (❍) μs upon 532 nm laser excitation under argon atmosphere.

However, in the present case, as it can be seen in Figure 4, the temporal profiles of the transient signals monitored at 340 and 460 for the Rudcbpy-UiO-67(Zr) MOF are different, supporting the occurrence of additional deactivation pathways, presumably a PET process competing with the emissive deactivation of the triplet excited state of Ru^{2+}. The temporal profiles of the transient signals monitored at 340, 460 and 600 nm, at long time scale after the laser pulse (Figure 5), are different indicating that they should correspond to at least two different transient species. The lifetimes of the transient species, obtained from the best fit of the temporal profiles to a mono-exponential or to a sum of two mono-exponential kinetics, have been calculated and summarized in Table 1. The fits are shown as red lines in Figure S9, for shorter-lived transient species (time scale 20 and 80 μs) and Figure 5, for longer-lived transient species (time scale 20,000 μs). The residuals of the lifetime calculations are listed in Table S1. It can be seen in this Table 1 that the photogenerated transient species are extremely long-lived, even longer than 18 ms, which is compatible with the generation of the charge separated state, but it is a time scale too long for electronic excited states. The transient signals are not quenched by O_2, indicating they could not come from a long-lived triplet excited state of the $Ru(bpy)_2$dcbpy linker. All the transient signals shown in Figure 5, completely decay to zero indicating that the photogenerated transient species return to the ground state. Thus, the transient signals could not come from an irreversible reaction. These observations can be rationalized assuming that the intersystem crossing deactivation of the triplet excited state of Ru^{2+} to the ground state competes with the PET process from the excited $Ru^{2+|3}$ to the MOF lattice, leading to the formation of a very long-lived (in the millisecond time scale) photoinduced charge

separated state. The photogeneration of long-lived charge separated states have been also previously observed for other related MOFs. [6,10,18,45-47] However, unlike other related MOFs, this Rudcbpy-UiO-67(Zr) MOF is able to photogenerate an extremely long-lived charge separated state upon excitation with long wavelength visible light irradiation. It is worth mentioning that the MOF is stable under the irradiation conditions with a 532 nm laser, as evidenced by the fact that the X-ray diffractogram of the material before and after the TAS measurements is the same, indicating that the crystal structure of the material remains intact under the irradiation conditions.

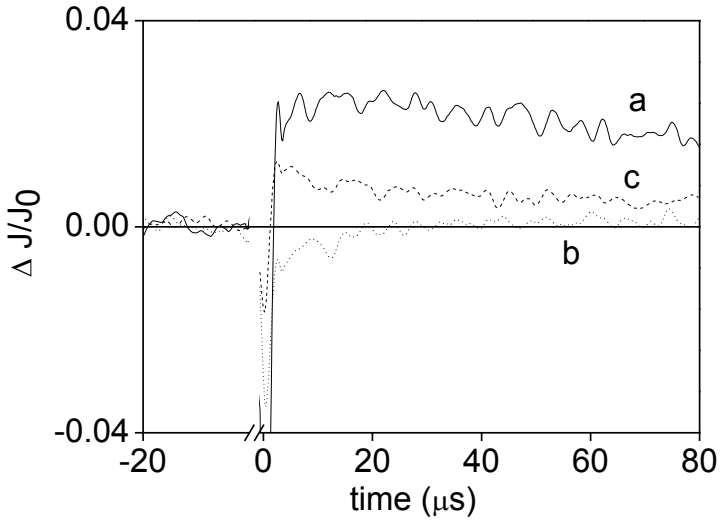

Figure 4. Temporal profiles of the signals monitored at 340 (a), 460 (b) and 600 (c) nm for Rudcbpy-UiO-67(Zr) MOF upon 532 nm laser excitation under argon atmosphere.

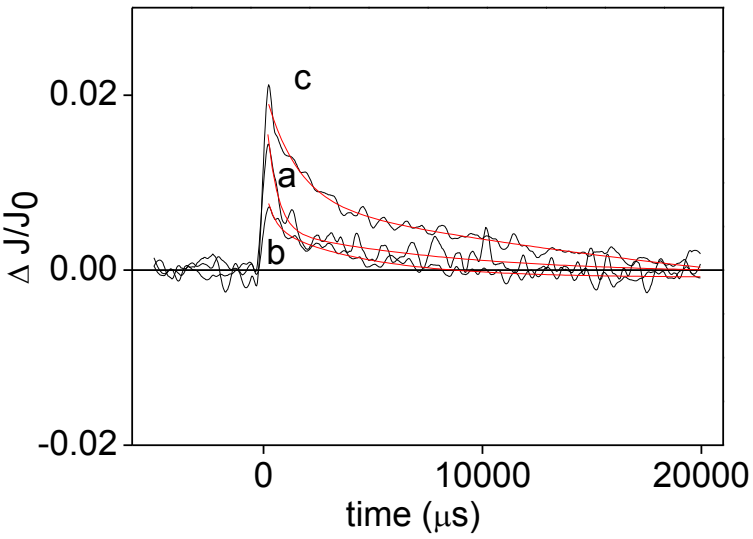

Figure 5. Temporal profiles of the signals monitored at 340 (a), 460 (b) and 600 (c) nm for Rudcbpy-UiO-67(Zr) MOF upon 532 nm laser excitation under argon atmosphere. The red line shows the best fit of the temporal profiles to a sum of two mono-exponential kinetics.

3.3 Quenching studies

To gain understanding about the nature of the photogenerated transient species upon 532 nm laser excitation, quenching experiments were performed. Figure S10 shows that N_2O, a well-known electron quencher with E (N_2O/N_2) = 1.36 V *vs* NHE,[48] completely quenches the transient signals monitored at 360 and 560 nm, while MeOH, a well-known hole quencher with E = 0.45-0.7 V vs NHE, does not quench or even increases the intensity of these transient signals. This behavior indicates that species responsible for the transient absorption spectrum recorded upon selective excitation of the Rudcbpy complex in the MOF (ground state E ($Ru^{3+/2+}$) = 1.5 V *vs* NHE, triplet oxidation potential of $Ru(bpy)_3^{2+}$ is -0.62 V) mainly corresponds to photoejected electrons with only a minor spectral contribution of positive holes.

Table 1. Lifetime of the transient species observed for Rudcbpy-UiO-67(Zr) obtained from the best fit of the temporal profiles to mono-exponential kinetics (exponential growth) for shorter-lived transient species (time scale 20 and 80 μs) or to a sum of two mono-exponential kinetics (exponential decay) for the longer-lived transient species (time scale 20000 μs).

Time scale (μs)	**Wavelength (nm)**	**τ(μs)**
20	600	0.668
80	460	11.8
20000	340	τ_1=477; τ_2= 8249
	460	τ_1=396; τ_2= 4450
	600	τ_1=1244;τ_2=18768

To discuss the feasibility of the proposed PET process and to determine the location of the photoejected electrons in the MOF lattice, TAS measurements of the Rudcbpy complex and the bpdc ligand in homogeneous solution were also performed to compare with the response of Rudcbpy-UiO-67(Zr). Upon 532 nm laser excitation of an aqueous solution of Rudcbpy complex, a transient absorption spectrum decaying in less than 1 μs, coincident with that previously reported,[35,41] was recorded (Figure S11). The lifetime of the triplet excited state of dissolved Rudcbpy complex was calculated as 0.022 μs from the best fit of the temporal profile of the transient signal monitored at 400 nm to a mono-exponential kinetics. This Rudcbpy triplet excited state is quenched by the addition of an aqueous solution of $Zr_6O_4(OH)_4$, (τ= 0.010 μs) (Figure S12) supporting the assumption that in Rudcbpy-UiO-67(Zr) the photogenerated triplet will be also quenched by the $Zr_6O_4(OH)_4$ nodes, probably even more efficiently. However, the transient signals monitored at 400, 460 and 715 nm do not change in the presence of an aqueous

solution of bpdc (Figure S13), supporting the lack of quenching of Rudcbpy triplet excited states in the MOF by this bpdc ligand. Addition of an aqueous solution of both, $Zr_6O_4(OH)_4$ and bpdc, in equimolar concentration causes the same quenching of the triplet excited state of the Rudcbpy complex as the addition of the $Zr_6O_4(OH)_4$ alone.

These results obtained from the homogeneous TAS measurements could be used to rationalized the photophysics occurring in the solid Rudcbpy-UiO-67(Zr) MOF. Thus, it is proposed that the triplet excited state of Ru^{2+} complex in the MOF should be able to transfer one electron to one of the Zr^{4+} ions of the inorganic cluster $Zr_6O_4(OH)_4$, but not to the biphenyldicarboxylate ligands of the MOF lattice. Accordingly, the PET process upon selective 532 nm laser excitation of the Rudcbpy-UiO-67(Zr) MOF should take place from the excited $Ru^{2+|3}$ of the Rudcbpy complex grafted to the MOF lattice to the inorganic cluster (see Scheme 1). To further confirm this proposal, an additional experiment was performed using UiO-67(Zr) as reference. Figure S14 shows the difference diffuse reflectance spectra between the UiO-67 MOF before and after the treatment with solid Mg as reducing agent. A continuous absorption spanning from 400 to 800 nm appears upon chemical reduction of UiO-67(Zr) MOF. This new absorption feature upon chemical reduction can be attributed to reduced zirconia clusters of UiO-67(Zr) MOF. It is expected that the redox potentials of the zirconia clusters are the same in both MOF UiO-67(Zr) and Rudcbpy-UiO-67(Zr), analogously to the invariability of the energetics of Rudcbpy complex incorporated into the UiO-67 MOF.[39] Therefore, it should also be possible to reduce the zirconia cluster in the Rudcbpy-UiO-67(Zr) MOF upon photoexcitation. Besides proving the possibility to reduce zirconia clusters in Rudcbpy-UiO-67(Zr) MOF, the Mg reduction allows to obtain the optical spectrum of the reduced zirconia clusters (Figure S14) that is similar to the TAS recorded at long times (500 μs) upon selective excitation of the Ru complex

in Rudcbpy-UiO-67(Zr) MOF, as it can be observed in the comparative Figure S16. This reference optical spectrum for reduced zirconia clusters supports the proposal of the occurrence of a PET process from excited $Ru^{2+|3}$ triplets of the Rudcbpy complex grafted to the MOF lattice to the inorganic zirconia cluster. It is worth mentioning that the TAS recorded at long times upon selective excitation of the Rudcbpy-UiO-67 MOF does not coincide exactly with the reference spectrum of the reduced zirconia clusters because in addition to photoejected electrons located in the inorganic $(Zr)_6O_4(OH)_4$ clusters, there should be other transient species, such as the positive hole located on the bpdc ligand or Ru species, that should contribute to the recorded TAS and whose absorption bands can overlap with those of the reduced zirconia cluster. The PET process from the organic linker to the inorganic cluster upon irradiation of the MOF has been previously reported for other type of MOF materials.[6,10,18,45]

The nature of the positive hole photogenerated after the PET process could be assigned, at first (20 μs) to the Ru^{3+} species, while there is still bleaching of the ground state, but the emission has disappeared. At long times after the laser pulse, 500 μs, when the bleaching of the Ru^{2+} complex is not further observed, it is reasonable to assume that there are no more Ru species involved in the transient signals. This means that the Ru^{3+} species has accepted one electron to return to the initial Ru^{2+} state. The observed shift in the maximum of the absorption band around 350 nm of the TAS recorded at long times could be related with the migration of the positive hole from the highly oxidizing Ru^{3+} species to the MOF lattice or to the water adsorbed molecules leading to a relocation of the positive hole at long times. The bpdc ligands of the MOF lattice are the most probable moieties being oxidized by the Ru^{3+} species, leading to a positive hole species located on these biphenyldicarboxylate units. For dissolved Rudcbpy complex, the back electron transfer should be very fast, leading to a charge separated state in the nanosecond time scale which does

not live long enough to be detected by our laser set-up. Thus, the appropriate way to record the TAS of the oxidized bpdc ligand is to irradiate the reference MOF without Rudcbpy complex, UiO-67(Zr), at 266 nm where the MOF absorbs light. Figure S15 shows the TAS of UiO-67(Zr) MOF upon 266 nm laser excitation. It has been recently reported for the UiO-66 MOF[47] that the PET process from the bpdc ligand to the inorganic cluster is not kinetically possible since there is no overlapping between the corresponding orbitals. Thus, the transient signal recorded when irradiating the UiO-67(Zr) at 266 nm should be correlated to the photogeneration of the oxidized bpdc ligand together with the solvated electron, most probably due to the presence of adsorbed H_2O on the MOF. It is well known in literature that the solvated electron in porous materials such as zeolites lives in the time scale of micro to milliseconds and the maximum absorption wavelength of its TAS depends on the chemical composition of the porous material in which it is photogenerated.[49-51] The TAS of the oxidized bpdc ligand, which is characterized by a continuous absorption in all the spectral range with higher absorption intensity at short wavelengths, is similar to the TAS recorded at long times, 500 μs, for the Rudcbpy-UiO-67(Zr) MOF upon 532 nm laser excitation (see comparative Figure S16). Analysis of the transient spectra of Rudcbpy-UiO-67(Zr) was made considering that it should be the sum of the absorption spectra of electrons and holes in Rudcbpy-UiO-67(Zr). The absorption spectrum of electrons in Rudcbpy-UiO-67(Zr) was considered to be the difference spectra after and before addition of Mg to UiO-67 (Zr). The absorption spectrum of holes located at the bpdc ligand in Rudcbpy-UiO-67(Zr) was assumed to be the transient spectrum of UiO-67(Zr) upon excitation at 266 nm. It was considered that under these conditions, charge separation occurs and electrons are quenched by coadsorbed water. This quenching could be further confirmed by looking at the TA spectrum of the dehydrated UiO-67 upon 266 nm in a non-polar organic solvent.[52] In spite of the relatively

poor resolution and the limited data points of the electron and holes spectra, the sum of the two agrees reasonable well with the transient spectrum of Rudcbpy-UiO-67(Zr). Figure S16 shows the comparison of the spectra calculated for the electron in the inorganic node and the positive hole in the bpdc ligand, the sum spectrum and the experimental spectrum recorded at long time after laser excitation. This analysis is compatible with our proposal of the occurrence of a PET process, competing with the emissive deactivation of the triplet excited state of Ru^{2+}. The PET process upon selective 532 nm laser excitation of the Rudcbpy-UiO-67 (Zr) MOF should take place from the triplet excited state of the Rudcbpy complex grafted to the MOF lattice to the inorganic cluster leading to a highly oxidizing Ru^{3+} transient species that returns to the ground state by oxidizing the bpdc ligands of the MOF lattice. It should be noted that the sum spectrum is not exactly the same as the experimental spectrum. Specifically, there is an absorption band between 350 and 450 nm in the sum spectra that seems not to be present in the experimental spectrum. This could be attributed to the fact that UiO-67(Zr) is taken for analysis of the transient spectra of Rudcbpy-UiO-67 (Zr) and the presence of the ruthenium complex could introduce additional spectral changes. Therefore, it should be also possible that the strongly oxidizing Ru^{3+} state decay also partly oxidizing adsorbed water molecules, in addition to the bpdc ligands. The lifetime of the charge separated state would be so long, because the positive hole and the electron are not geminate and should eventually recombine separately.

3.4 Generation of methyl viologen radical cation

The steady-state 532 nm laser irradiation of an acetonitrile suspension of the Rudcbpy-UiO-67(Zr) MOF in the presence of methyl viologen, MV^{2+}, as electron acceptor, and TEOA as

sacrificial electron donor, gives rise to the formation of the methyl viologen radical cation, $MV^{\cdot+}$, which can be visually observed by the appearance of its characteristic blue color.[30,53] This indicates that upon visible light irradiation a PET process from the photoexcited Rudcbpy-UiO-67(Zr) MOF to the MV^{2+} has occurred when a source of electrons as TEOA is present (Figure 6). Blank controls have been performed showing that $MV^{\cdot+}$ is not generated in the dark or upon irradiation in the absence of TEOA. In contrast, the $MV^{\cdot+}$ can be generated upon irradiation: i) employing the Rudcbpy complex, as reference, ii) employing UiO-67(Zr) MOF instead of Rudcbpy-UiO-67(Zr) MOF, and iii) in the absence of Rudcbpy-UiO-67(Zr) MOF, when only MV^{2+} and TEOA are present in the medium. Low concentrations of $MV^{\cdot+}$ were detected in blank controls ii and iii, indicating some degree of spontaneous chemical reduction of MV^{2+} by TEOA. In these blank controls, TEOA is the reducing chemical agent and reduces MV^{2+} directly. In the experiments where Rudcbpy-UiO-67(Zr) MOF or Rudcbpy complex were uses as photosensitizers and MV^{2+} and TEOA are present, the $MV^{\cdot+}$ concentration measured upon irradiation was much higher. The prevalent process is proposed to be a PET process from the photoexcited Rudcbpy-UiO-67(Zr) MOF or Rudcbpy complex to the MV^{2+} when a sacrificial electron donor TEOA is present, accompanied by a lesser contribution of the direct chemical reduction of MV^{2+} by TEOA.

The UV-vis absorption spectra recorded for most of these assays showed the characteristic absorption bands of the $MV^{\cdot+}$, a sharp and intense absorption band at 390 nm and a broad and less intense structured absorption band centered at about 600 nm (Figure 6). The concentration of the photogenerated $MV^{\cdot+}$ in the different experiments could be calculated by using the reported extinction coefficient of $MV^{\cdot+}$ at 600 nm,[54] and subtracting the low concentration of the $MV^{\cdot+}$

radical cation obtained in the blank experiment iii, when only MV^{2+} and TEOA are present. Table 2 summarizes the data obtained.

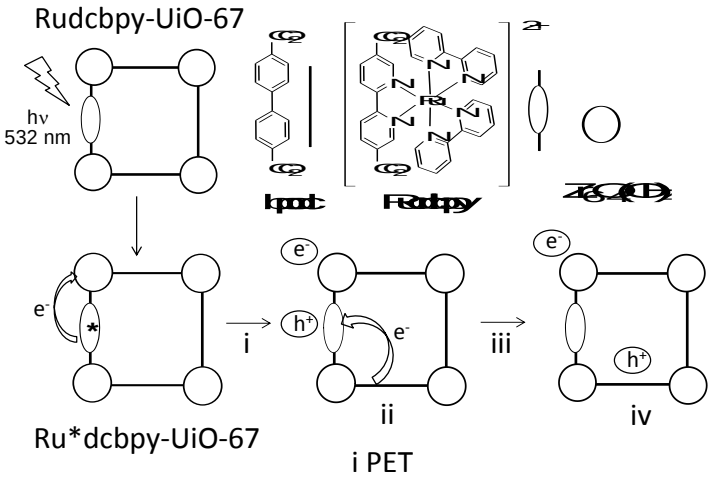

Scheme 1. Proposed PET process upon 532 nm laser excitation of the Rudcbpy-UiO-67(Zr) MOF.

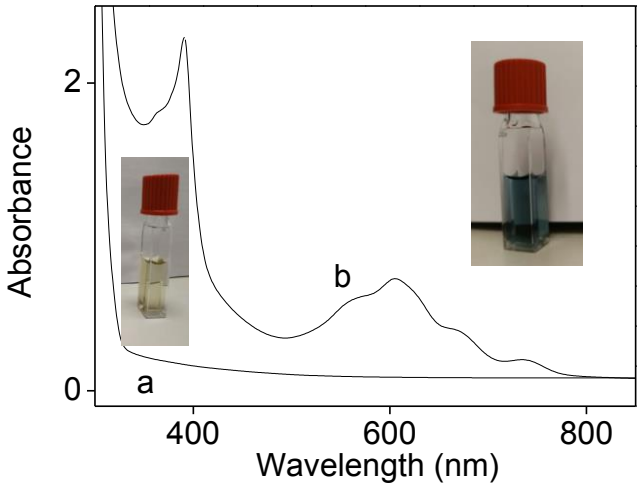

Figure 6. UV-vis absorption spectra of an acetonitrile suspension of the Rudcbpy-UiO-67(Zr) MOF in the presence of MV^{2+}, as electron acceptor, and TEOA, as sacrificial electron donor before (a) and after (b) 532 nm laser irradiation. The photographs show the real color of the solutions under each condition.

An acetonitrile suspension of the Rudcbpy-UiO-67(Zr) solid MOF in the presence of MV^{2+} and TEOA was prepared under the same experimental conditions employed for the photogeneration of $MV^{\cdot+}$ radical cation. Before irradiation, the Rudcbpy-UiO-67 solid MOF was centrifuged from the mixture and the UV-vis spectrum of the supernatant solution was recorded (Figure S17). No absorption band at 450 nm attributable to the Rudcbpy complex could be observed. Furthermore, ICP analysis of the supernatant solution reveals that the Ru leaching from the MOF to the solution was negligible (0.22 % Ru of the initial Ru content of Rudcbpy-UiO-67(Zr)), thus indicating the stability and robustness of the Rudcbpy-UiO-67(Zr) MOF in the presence of TEOA. The stability of the MOF under the 532 nm laser irradiation conditions has been previously established when commenting the TAS measurements.

Then, taking into account that the solutions containing the Rudcbpy-UiO-67(Zr) MOF and the Rudcbpy complex were matched to the same absorbance at the irradiation wavelength (532 nm) and have been prepared under the same experimental conditions, the concentration of the photogenerated $MV^{\cdot+}$ could be indicative of the efficiency of the PET process from the photoexcited Ru^{2+} to the MV^{2+}. It should be noted that the amount of MOF employed to prepare the suspension is very small and that this suspension was sonicated for 15 min before measuring the UV-Vis spectrum. These conditions minimize light scattering and allows sufficient

transmittance for ensuring reliable measurements in the transmission mode. It has been calculated that the PET process from the photoexcited Rudcbpy-UiO-67(Zr) MOF to the MV^{2+} was 26 % with respect to that from the homogeneous complex Rudcbpy. This decrease in the PET efficiency is probably a reflection of diffusion limitations as consequence of immobilization of Rudcbpy complex in the structure of the UiO-67 MOF, or due to MV^{2+} diffusion limitations into and through the bulk of the MOF crystallite and its restricted access to Ru complexes in the MOF bulk or due to the less efficient light absorption by the anchored Ru complex due to light scattering.

Table 2. Concentration of the photogenerated $MV^{\cdot+}$ radical cation in the different experiments under 532 nm laser irradiation for 10 minutes, calculated by using the reported extinction coefficient of the 600 nm absorption band (ε = 13900 $M^{-1}cm^{-1}$ from ref 54) and subtracting the concentration of the $MV^{\cdot+}$ obtained in the blank experiment when only MV^{2+} and TEOA are present.

Photocatalyst	$[MV^{\cdot+}]$ (μM)
UiO-67(Zr)	0
Rudcbpy-UiO-67(Zr)	12.3
Rudcbpy	48.3

3.5 Photoredox activity

Understanding of the photophysics occurring in this system has been employed to perform the photocatalytic debromination of α-bromoacetophenone (**1**).[27,55] Control experiment in the presence of Rudcbpy-UiO-67(Zr) in the dark does not show any conversion. Similarly, treating compound **1** with TEOA under UV-visible light irradiation in the absence of Rudcbpy-UiO-67(Zr) leads to the formation of acetophenone (**2**) with a yield about 10 % at 2 h. In contrast, when Rudcbpy-UiO-67(Zr) was present at 1 mol% together with TEOA and the mixture was irradiated with UV-visible light conversion of substrate **1** over 90 % yielding exclusively compound 2 was observed (Scheme 2). The yield of the debromination reaction of 2-bromoacetophenone using UiO-67 MOF as photocatalyst instead of Rudcbpy-UiO-67 MOF was approximately the same as the one obtained for the blank control in the absence of photocatalyst, thus indicating that the UV absorption of the UiO-67 MOF does not contribute significantly to the photocatalytic activity of the Rudcbpy-UiO-67 MOF.

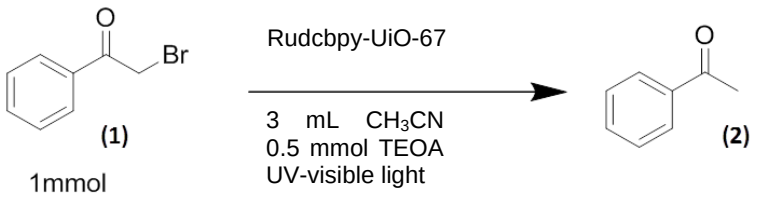

Scheme 2. Debromination reaction of 2-bromoacetophenone using Rudcbpy-UiO-67(Zr).

Figure 7 shows the temporal evolution of the photoredox debromination compared to the controls. An additional experiment was performed to determine the photocatalytic activity of Rudcbpy complex as homogeneous photocatalyst at the same concentration and the results are also plotted in Figure 7. It can be seen there that the reaction rate of the homogeneous Ru(II) complex was much lower than that measured for the heterogeneous Rudcbpy-UiO-67(Zr). According to the previous characterization of the transients involved in the process, it seems that

the long lifetime of the charge separation states for the complex attached to the UiO-67(Zr) structure is the main factor justifying the higher efficiency of the heterogeneous version of the photoredox debromination.

When using solid catalyst two issues that should be addressed are to prove the heterogeneity of the process and the stability of the material. To demonstrate the heterogeneity of the photoredox reaction using Rubcdpy-UiO-67(Zr) as solid photocatalyst, two twin experiments were performed under the optimal conditions. In one experiment, the solid photocatalyst was removed at 10 minutes reaction time, when conversion reached 25 %. In the other experiment the photocatalyst was present during the complete reaction time. The results are presented in Figure 8. It was observed that while the reaction in the presence of solid catalyst reached almost complete conversion at 2 h, filtration of the solid 10 minutes after starting the reaction stops completely the debromination reaction, showing that it is the solid material the active photocatalyst for the transformation. To further confirm the heterogeneity of the process and the stability of the MOF under the reaction conditions, two additional tests were performed. The UV-Vis spectrum of the filtered solution was recorded (Figure S18), whereby no absorption bands attributable to the Rudcbpy complex were observed. ICP analysis of the filtered solution revealed that Ru leaching from the MOF to the solution was 0.15% Ru of the initial Ru content in the MOF, thus indicating the stability and robustness of the Rudcbpy-UiO-67 MOF under the photoreaction conditions.

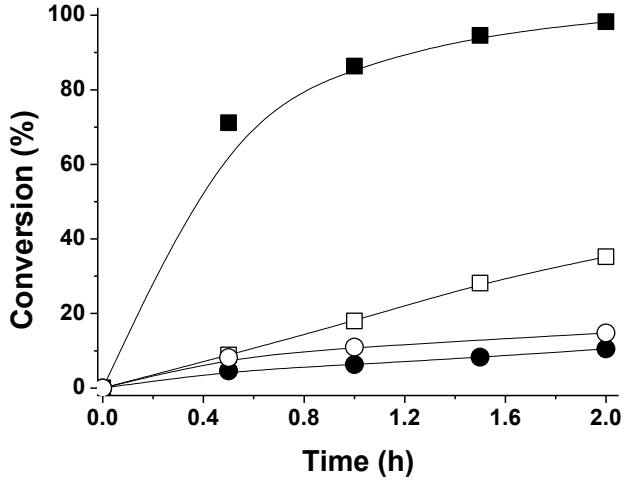

Figure 7. Time-Conversion plot for the debromination reaction of 2-bromoacetophenone (**1**) to acetophenone (**2**) using (■) Rubcdpy-UiO-67(Zr), (□) Rubcdpy, (○) cis-dichlorobis(2,2'-bipyridine) Ruthenium (II) and (●) blank control. Reaction conditions: catalyst (0.2 mol% of Ru), substrate (1 mmol), 3 mL CH_3CN, 0.5 mmol TEOA and UV-Visible light.

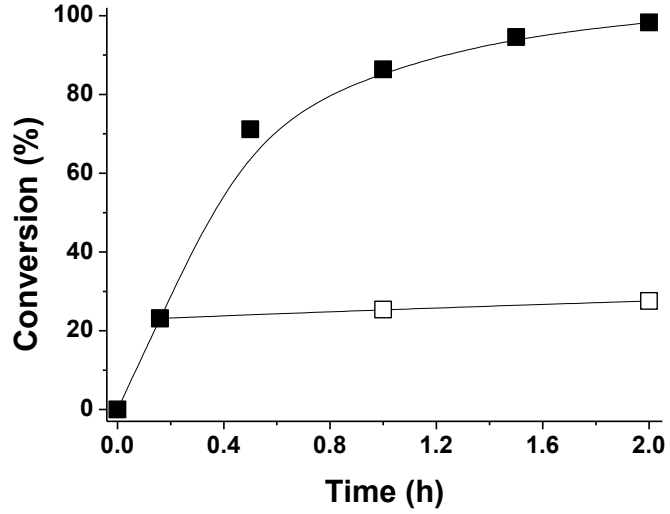

Figure 8. Time-Conversion plot for the debromination reaction of 2-bromoacetophenone (**1**) to acetophenone (**2**) using (■) Rubcdpy-UiO-67(Zr) as catalyst that is filtered at 10 min reaction

time (□). Reaction conditions: catalyst (0.2 mol% of Ru), substrate (1 mmol), 3 mL CH_3CN, 0.5 mmol TEOA and UV-Visible light.

Stability of Rubcdpy-UiO-67(Zr) was supported by performing a series of consecutive uses of the same sample following the temporal profile of the photodebromination and checking the crystallinity of the MOF after extensive use. The results are presented in Figure 9. Very similar initial reaction rates, temporal evolutions and final conversions were observed after three consecutive uses of the same Rubcdpy-UiO-67(Zr), indicating that the photocatalytic activity is not decreased by deactivation of the material. The minor differences in the temporal profile could be due to unavailable losses of some material during the recycling work up. XRD of the solid after three consecutive uses exhibits the same pattern as that of the fresh material confirming that the crystal structure of UiO-67(Zr) is completely preserved in the photocatalytic reaction. This stability is in accordance with the robustness of UiO-67(Zr) structure generally reported under various reaction conditions.

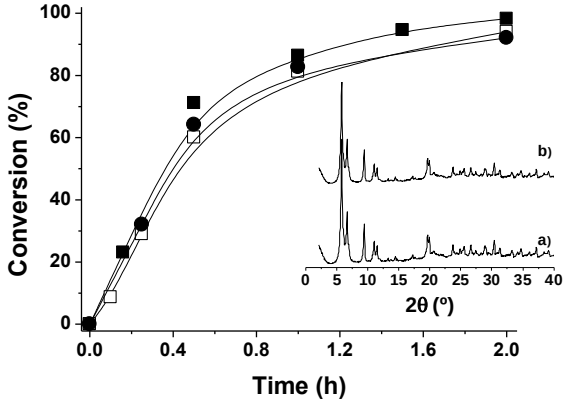

Figure 9. Reusability experiments using Rubcdpy-UiO-67(Zr) as catalyst in the debromination reaction of 2-bromoacetophenone (**1**) to acetophenone (**2**). Reaction conditions: catalyst (0.2 mol% of Ru), substrate (1 mmol), 3 mL CH_3CN, 0.5 mmol TEOA and UV-Visible light. Legend:

1st (■), 2nd (□) and 3rd use (●). Inset: XRD of fresh Rubcdpy-UiO-67(Zr) (a) and Rubcdpy-UiO-67(Zr) used three times (b).

Based on the previous characterization of the charge separation state and the quenching studies with sacrificial electron donor, the photodebromination mechanism indicated in Scheme 3 is proposed. After light absorption by the Rudcbpy unit and generation of the charge separation, electron transfer to compound **1** would generate bromide and α-ketomethyl radical that could undergo a second electron transfer before diffusing outside the MOF pores resulting in the corresponding enolate that after protonation would form acetophenone (**2**). The photochemical cycle is closed by the tertiary amine acting as electron donor restoring the Rudcbpy-UiO-67(Zr) to the initial state. This proposal is in agreement with related precedents on homogeneous photoredox reactions.[27,55]

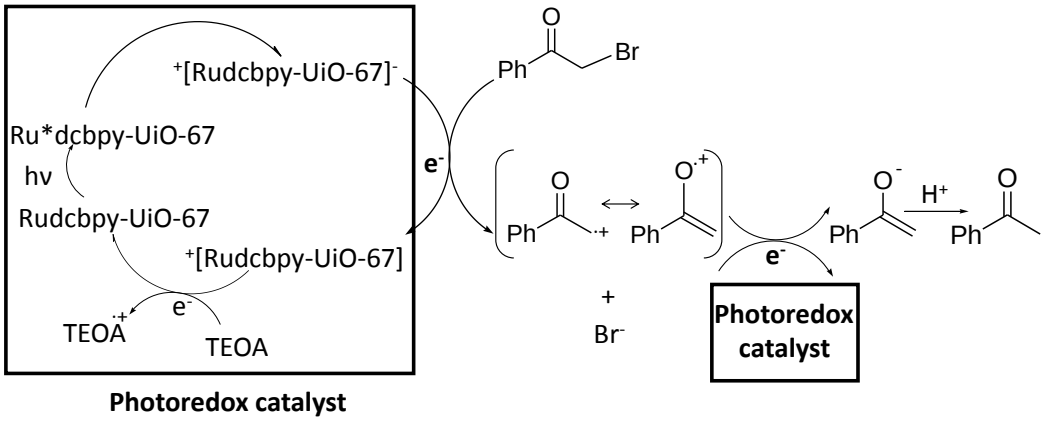

Scheme 3. Proposed photodebromination mechanism of 2-bromoacetophenone (**1**) using Rudcbpy-UiO-67(Zr).

4. CONCLUSIONS

Even though Rudcbpy-UiO-67(Zr) has attracted considerable attention as photocatalyst, photophysical studies on this material reported so far have been based on photoluminescence studies that only report on the emissive triplet excited state of the anchored Ru complex. By using TAS, spectroscopic evidence in support of the occurrence of a PET process from the excited Ru^{2+*} triplet to the MOF lattice in Rudcbpy-UiO-67(Zr) upon visible light irradiation has been obtained. This PET leads to the generation of a previously undetected long-lived (milliseconds) charge separation state. Analogous TAS measurements for the soluble Rudcbpy complex in water support the assignment of the photogenerated charge separated species to photoejected electrons, located on the inorganic cluster $Zr_6O_4(OH)_4$, and to positive holes, located on Ru^{3+} species, for the first 20 microseconds after the laser pulse, and, then, migrating to the MOF lattice or reacting with H_2O molecules. The occurrence of PET was firmly demonstrated by the visual observation of the generation and growth of $MV^{\cdot+}$ radical cation that was characterized by steady-state spectroscopy. The long lifetime of the photoinduced charged separated state has been postulated to be advantageous for the efficient photocatalytic debromination of α-bromoacetophenone using a tertiary amine as reductant sacrificial agent, following a photoredox mechanism. Rudcbpy-UiO-67(Zr) acts as a heterogeneous photocatalyst and can be reused without decreasing the catalytic activity or changes in the structure of the material.

ASSOCIATED CONTENT

Supporting Information. A listing of the contents of each file supplied as Supporting Information should be included. For instructions on what should be included in the Supporting

Information as well as how to prepare this material for publications, refer to the journal's Instructions for Authors.

AUTHOR INFORMATION

Corresponding Author

* E-mail: hgarcia@qim.upv.es; bferrer@qim.upv.es

Author Contributions

A. Santiago-Portillo prepared the materials and carried out photodebromination. H. G. Baldoví and B. Ferrer measured TAS. E. Carbonell performed the MV^{2+} experiments. M. Alvaro characterized the materials. B. Ferrer and H. Garcia conceived the research. The manuscript was written through contributions of all authors. All authors have given approval to the final version of the manuscript.

ACKNOWLEDGMENT

Financial support by the Spanish Ministry of Economy and Competitiveness (CTQ2014-53292-R-AR, Severo Ochoa, CTQ2015-69153-CO_2-R) and Generalitat Valenciana (Prometeo 2017/083) is gratefully acknowledged. S.N. thanks financial support by Fundación Ramón Areces (XVIII Concurso Nacional, Ciencias de la Vida y de la Materia, Energía renovable: materiales y procesos 2016).

REFERENCES

(1) Stock, N.; Biswas, S. Synthesis of Metal-Organic Frameworks (MOFs): Routes to Various MOF Topologies, Morphologies, and Composites. *Chem. Rev.* **2012**, *112*, 933-969.

(2) O'Keeffe, M. Design of MOFs and Intellectual Content in Reticular Chemistry: A Personal View. *Chem. Soc. Rev.* **2009**, *38*, 1215-1217.

(3) Rowsell, J. L. C.; Yaghi, O. M. Metal-Organic Frameworks: A New Class of Porous Materials. *Micropor. Mesopor. Mater.* **2004**, *73*, 3-14.

(4) Furukawa, H.; Cordova, K.E.; O'Keeffe, M.; Yaghi, O. M.; The Chemistry and Applications of Metal-Organic Frameworks. *Science* **2013**, *341*, 1230444.

(5) Férey, G. Hybrid Porous Solid: Past, Present, Future. *Chem. Soc. Rev.* **2008**, *37*, 191-214

(6) Alvaro, M.; Carbonell, E.; Ferrer, B.; Llabrés i Xamena, F. X.; Garcia, H.; Semiconductor Behaviour of a Metal-Organic Framework (MOF). *Chem.-Eur.J.* **2007**, *13*, 5106-5112.

(7) Bordiga, S.; Lamberti, C.; Ricchiardi, G.; Regli, L.; Bonino, F.; Damin, A.; Lillerud, K. P.; Bjorgen, M.; Zecchina, A. Electronic and Vibrational Properties of a MOF-5 Metal-Organic Framework: ZnO Quantum Dot Behaviour. *Chem. Commun.,* **2004**, *20*, 2300-2301.

(8) Ramamurthy, V.; Shailaja, J.; Kaanumalle, Lakshmi S.; Sunoj, R. B.; Chandrasekhar, J. Controlling Chemistry with Cations: Photochemistry within Zeolites. *Chem. Commun.* **2003**, *0*, 1987–1999.

(9) Llabrés i Xamena, F. X.; Corma, A.; Garcia, H. Applications for Metal-Organic Frameworks (MOFs) as Quantum Dot Semiconductors. *J. Phys. Chem. C*, **2007**, *111*, 80-85.

(10) Lopez, H. A.; Dhakshinamoorthy, A.; Ferrer, B.; Atienzar, P.; Alvaro, M.; Garcia, H. Photochemical Response of Commercial MOFs: $Al_2(BDC)_3$ and Its Use As Active Material in Photovoltaic Devices. *J. Phys. Chem. C*, **2011**, *115*, 22200-22206.

(11) Silva, C. G.; Corma, A.; Garcia, H. Metal-Organic Frameworks as Semiconductors. *J. Mater. Chem.* **2010**, *20*, 3141-3156.

(12) Lee, D. Y.; Kim, E. K.; Shin, C. Y.; Shinde, D. V.; Lee, W.; Shrestha, N. K.; Lee, J. K.; Han, S. H. Layer-by-Layer Deposition and Photovoltaic Property of Ru-Based Metal-Organic Frameworks. *RSC Adv.,* **2014**, *4*, 12037-12042.

(13) Leong, K.; Foster, M. E.; Wong, B. M.; Spoerke, E. D.; van Gough, D.; Deaton, J. C.; Allendorf, M. D. Energy and Charge Transfer by Bonor-Acceptor Pairs Confined in a Metal-

Organic Framework: A spectroscopic and Computational Investigation. *J. Mater. Chem. A,* **2014**, *2*, 3389-3398.

(14) Stavila, V.; Talin, A. A.; Allendorf, M. D. MOF-Based Electronic and Opto-electronic Devices. *Chem. Soc. Rev.,* **2014**, *43*, 5994-6010.

(15) Lin, S.; Pineda-Galvan, Y.; Maza, W. A.; Epley, C.C.; Zhu, J.; Kessinger, M.C.; Pushkar, Y.; Morris, A. J. Electrochemical Water Oxidation by a Catalyst-Modified Metal-Organic Framework Thin Film. *ChemSusChem,* **2017,** *10*, 514-522.

(16) Padilla, R.; Maza, W. A.; Dominijannic, A. J.; Winkel, B. S. J.; Morris, A. J.; Brewer, K. J. Pushing the Limits of Structurally-Diverse Light-Harvesting Ru (II) Metal-Organic Chromophores for Photodynamic Therapy. *J. Photochem. and Photobiol. A: Chemistry,* **2016**, *322–323*, 67-75.

(17) Barrett, S. M.; Wang, C.; Lin, W. Oxygen Sensing *via* Phosphorescence Quenching of Doped Metal-Organic Frameworks. *J. Mater. Chem.,* **2012**, *22*, 10329-10334.

(18) Ferrer, B.; Alvaro, M.; Baldovi, H. G.; Reinsch, H.; Stock, N. Photophysical Evidence of Charge-Transfer-Complex Pairs in Mixed-Linker 5-Amino/5-Nitroisophthalate CAU-10. *ChemPhysChem,* **2014**, *15,* 924-928.

(19) Wang, C. C.; Li, J. R.; Lv, X. L.; Zhang, Y. Q.; Guo, G. Photocatalytic Organic Pollutants Degradation in Metal-Organic Frameworks. *Energ. Environ. Sci.,* **2014**, *7*, 2831-2867.

(20) Wu, Z.; Yuan, X.; Zhang, J.; Wang, H.; Jiang, L.; Zeng, G. Photocatalytic Decontamination of Wastewater Containing Organic Dyes by Metal-Organic Frameworks and their Derivatives. *ChemCatChem,* **2017**, *9*, 41-64.

(21) Dhakshinamoorthy, A.; Asiri, A. M.; García, H. Metal-Organic Frameworks (MOF) Compounds: Photocatalysts Redox Reaction and Solar Fuel Production. *Angew. Chem. Int. Ed.,* **2016**, *55*, 5414-5445.

(22) Li, S. L.; Xu, Q. Metal-Organic Frameworks as Platforms for Clean Energy. *Energ. Environ. Sci.,* **2013**, *6*, 1656-1683.

(23) Zeng, L.; Guo, X.; He, C.; Duan, C. Metal-Organic Frameworks: Versatile Materials for Heterogeneous Photocatalysis. *ACS Catal.,* **2016**, *6*, 7935-7947.

(24) Zhang, T.; Lin, W. Metal-Organic Frameworks for Artificial Photosynthesis and Photocatalysis. *Chem. Soc. Rev.,* **2014**, *43*, 5982-5993.

(25) Deng, X.; Li, Z.; García, H.; Frontispiece: Visible Light Induced Organic Transformations Using Metal-Organic-Frameworks (MOFs). *Chem.-Eur.J.,* **2017**, *23*, 11189-11209.

(26) Yu, X.; L. Wang, S. M. Cohen, Photocatalytic Metal-Organic Frameworks for Organic Transformations. *CrystEngComm,* **2017**, *19*, 4126-4136.

(27) Prier, C. K.; Rankic, D. A.; MacMillan, D. W. C. Visible Light Photoredox Catalysis with Transition Metal Complexes: Applications in Organic Synthesis. *Chem. Rev.,* **2013**, *113*, 5322-5363.

(28) Balzani, V.; Scandola, F. Supramolecular Photochemistry, Ellis Horwood: Chichester, England, **1991**.

(29) Harriman, A.; Ziessel, R. Building Photoactive Molecular-Scale Wires. *Coord. Chem. Rev.,* **1998**, *171*, 331-339.

(30) Álvaro, M.; Carbonell, E.; Ferrer, B.; García, H.; Herance, J. R. Ionic Liquids as a Novel Medium for Photochemical Reactions. $Ru(bpy)_3^{2+}$/Viologen in Imidazolium Ionic Liquid as a Photocatalytic System Mimicking the Oxido-Reductase Enzyme. *Photochemistry and Photobiology*, **2006**, *82*, 185-190.

(31) Narayanam, J. M. R.; Stephenson, C. R. J. Visible Light Photoredox Catalysis: Applications in Organic Synthesis. *Chem Soc. Rev.* **2011,** *40*, 102-113.

(32) Font, J.; de March, P.; Busque, F.; Casas, E.; Benitez, M.; Teruel, L.; García, H. Periodic Mesoporous Silica having Covalently Attached tris(bipyridine)Ruthenium Complex: Synthesis, Photovoltaic and Electrochemiluminescent Properties, *J. Mater. Chem.,* **2007**, *17*, 2336-2343.

(33) Zhang, H.; Rajesh, Ch. S.; Dutta, P. K. Visible-Light-Driven Photoreactions of $[(bpy)_2Ru(II)L]Cl_2$ in Aqueous Solutions (bpy = Bipyridine, L = 1,2-Bis(4-(4'-methyl)-2,2'-bipyridyl)Ethene),. *J. Phys. Chem. C.* **2009**, *113*, 4623-4633.

(34) Park, Y. S.; Lee, E. J.; Chun, Y. S.; Yoon, Y. D.; Yoon, K. B. Long-Lived Charge-Separation by Retarding Reverse Flow of Charge-Balancing Cation and Zeolite-Encapsulated $Ru(bpy)_3^{2+}$ as Photosensitized Electron Pump from Zeolite Framework to Externally Placed Viologen. *J. Am. Chem. Soc.* **2002**, *124*, 7123-7135.

(35) Farnum, B. H.; Morseth, Z. A.; Lapides, A. M.; Rieth, A. J.; Hoertz, P. G. M.; Brennaman, K.; Papanikolas, J. M.; Meyer, T. J. Photoinduced Interfacial Electron Transfer within a Mesoporous Transparent Conducting Oxide Film. *J. Am. Chem. Soc.* **2014**, *136*, 2208-2211.

(36) Wang, C.; Xie, Z.; de Krafft, K. E.; Lin, W. Doping Metal-Organic Frameworks for Water Oxidation, Carbon Dioxide Reduction, and Organic Photocatalysis. *J. Am. Chem. Soc.* **2011**, *133*, 13445-13454.

(37) Maza W. A.; Morris, A. J. Photophysical Characterization of a Ruthenium (II) Tris(2,2'-bipyridine)-Doped Zirconium UiO-67 Metal-Organic Framework. *J. Phys. Chem. C,* **2014**, *118*, 8803-8817.

(38) Maza, W. A.; Ahrenholtz, S. R.; Epley, C. C.; Day, C. S.; Morris, A. J. Solvotermal Growth and Photophysical Characterization of a Ruthenium(II) Tris(2,2'-Bipyridine)-Doped Zirconium UiO-67 Metal Organic Framework Thin Film. *J. Phys. Chem. C,* **2014**, *118*, 14200-14210.

(39) Maza, W. A.; Haring, A. J.; Ahrenholtz, S. R.; Epley, C. C.; Lin, S. Y.; Morris, A. J. Ruthenium (II)-polypyridyl Zirconium (IV) Metal-Organic Frameworks as a New Class of Sensitized Solar Cells. *Chem. Sci.,* **2016**, *7*, 719-727.

(40) Zhu, J.; Maza, W. A.; Morris, A. J. Light-Harvesting and Energy Transfer in Ruthenium (II)-polypyridyl Doped Zirconium(IV) Metal-Organic Frameworks: A Look Toward Solar Cell Applications. *J. Photochem. and Photobiol. A: Chemistry,* **2017,** *344*, 64–77.

(41) Hou, C. C.; Li, T. T.; Cao, S.; Chen, Y.; Fu, W. F. Incorporation of a $[Ru(dcbpy)(bpy)_2]^{2+}$ Photosensitizer and a $Pt(dcbpy)Cl_2$ Catalyst into Metal-Organic Frameworks for Photocatalytic Hydrogen Evolution from Aqueous Solution. *J. Mater. Chem. A,* **2015**, *3*, 10386-10394.

(42) Wang, J. L.; Wang, C.; Lin, W. Metal-Organic Frameworks for Light Harvesting and Photocatalysis. *ACS Catal.,* **2012,** *2*, 2630-2640.

(43) Sullivan, B. P.; Salmon, D. J.; Meyer, T. J. Mixed Phosphine 2,2'-bipyridine Complexes of Ruthenium. *J. Inorg. Chem.* **1978**, *17*, 3334−3341.

(44) Xie, P. H.; Hou, Y. J.; Zhang, B. W.; Cao, Y.; Wu, F.; Tian, W. J.; Shen, J. C. Spectroscopic and Electrochemical Properties of Ruthenium (II) polypyridyl Complexes. *J. Chem. Soc., Dalton Trans.,* **1999**, 4217–4221.

(45) Santiago Portillo, A.; Baldoví, H. G.; García Fernandez, M. T.: Navalón, S.; Atienzar, P.; Ferrer, B.; Alvaro, M.; Garcia, H.; Li, Z. Ti as Mediator in the Photoinduced Electron Transfer of Mixed-Metal NH_2-UiO-66(Zr/Ti): Transient Absorption Spectroscopy Study and Applications in Photovoltaic Cell. *J Phys Chem C,* **2017**, *121*, 7015-7024.

(46) Dan-Hardi, M.; Serre, C.; Frot, T.; Rozes, L.; Maurin, G.; Sanchez, C.; Ferey, G. A New Photoactive Crystalline Highly Porous Titanium(IV) Dicarboxylate. *J. Am. Chem. Soc.* **2009**, *131*, 10857-10859.

(47) Nasalevich, M. A.; Hendon, C. H.; Santaclara, J. G.; Svane, K.; van der Linden, B.; Veber, S. L.; Fedin, M. V.; Houtepen, A. J.; van der Veen, M. A.; Kapteijn F. et Al, Electronic Origins of Photocatalytic Activity in d^0 Metal Organic Frameworks. *Sci Rep,* **2016**, *6*, 23676.

(48) Handbook of Organic Photochemistry, (Ed. J. C. Scaiano) CRC Press, Boca Raton, FL., **1989**.

(49) Ellison, E. H. Electron Trapping in Polar-Solvated Zeolites. *J. Phys. Chem. B*, **2005**, *109*, 20424-20432

(50) Álvaro, M.; Ferrer, B; Fornés, V; García, H. A Periodic Mesoporous Organosilica Containing Electron Acceptor Viologen Units. *Chem. Commun.,* **2001**, 2546–2547.

(51) Álvaro, M.; Chretien, M. N.; Ferrer, B; Fornés, V; García, H.; Scaiano, J. C. First Molecular Switch Encapsulated within the Cavities of a Zeolite. A Dramatic Lifetime Increase of the Charge-Separated State. *Chem. Commun.,* **2001**, 2106–2107.

(52) Shearer, G. C.; Forselv, S.; Sachin Chavan, S.; Bordiga, S.; Mathisen, K.; Bjørgen, M.; • Svelle, S.;Lillerud, K. P. In Situ Infrared Spectroscopic and Gravimetric Characterisation of the Solvent Removal and Dehydroxylation of the Metal Organic Frameworks UiO-66 and UiO-67. *Top Catal.* **2013**, *56*, 770–782.

(53) Jose Raul Herance,J. R., Ferrer,B., Bourdelande,J. L., Marquet, J., Garcia, H. A Photocatalytic Acid- and Base-Free Meerwein–Ponndorf–Verley-Type Reduction Using a $[Ru(bpy)_3]^{2+}$/Viologen Couple. *Chem. Eur. J.* **2006**, *12*, 3890 – 3895

(54) Watanabe, T.; Honda, K. Measurement of the Extinction Coefficient of the Methyl Viologen Cation Radical and the Efficiency of its Formation by Semiconductor Photocalysis. *J. Phys. Chem.,* **1982**, *86*, 2617-2619.

(55) Yoon, T. P.; Ischay, M. A.; Du, J. Visible Light Photocatalysis as a Greener Approach to Photochemical Synthesis. *Nature Chemistry*, **2010,** *2*, 527–532.

TOC graphic

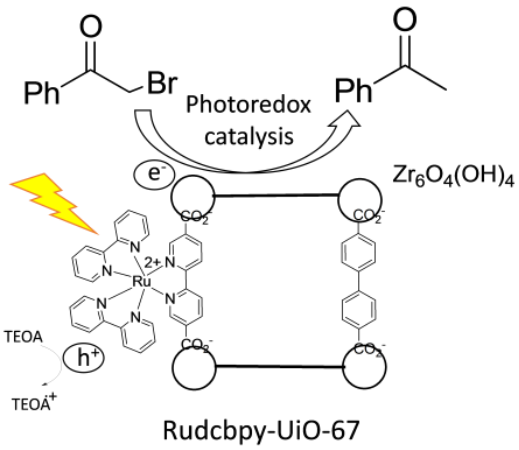
O
Ph
Br
Photoredox
catalysis
O
Ph
$Zr_6O_4(OH)_4$
e^-
CO_2^-
2+
Ru
N
TEOA
h^+
TEOA$^+$
Rudcbpy-UiO-67